



Cite this: *Chem. Commun.*, 2025, 61, 13461

Received 12th March 2025,  
Accepted 1st August 2025

DOI: 10.1039/d5cc01356a

[rsc.li/chemcomm](http://rsc.li/chemcomm)

**Integration of a photocathode,  $\text{CoCpCp}^*$ , and a heterogenized rhenium catalyst within PCN-777 provides stable photocurrent and CO as the product of photo-driven  $\text{CO}_2$  reduction. Control experiments confirm the role of  $\text{CoCpCp}^*$  as redox mediator. This proof-of-concept study illustrates the feasibility of using MOF-embedded molecular catalysts in DS-PEC systems.**

Photoelectrochemical cells (PECs) can harness sunlight to drive the formation of renewable fuels (solar fuels).<sup>1</sup> These PECs are multicomponent systems, in the sense that they require light-absorbing materials, electron-transporting materials and catalytic materials bundled within one device. The first two aspects could principally be covered using semiconductor materials. However, most semiconductors are inefficient due to limited light harvesting properties, particularly in the visible part of the solar spectrum, which is linked to the large bandgap in these materials.<sup>2</sup> Dye-sensitized solar cells (DSSC) are comprised of a molecular photosensitizer onto a semiconductor, which enables the efficient absorption of solar energy.<sup>3</sup> DSSC's contain a redox couple for dye regeneration and circuit closure, they exhibit good performance under diffuse light conditions and are cheap to produce.<sup>4</sup> Combining a DSSC set-up with a molecular catalyst instead of a redox couple creates a device known as a dye-sensitized photoelectrochemical cell (DS-PEC), sometimes referred to as an artificial photosynthesis device, which may facilitate a chemical reaction. Over the past decades, significant progress in the field of solar fuels has been made, particularly in the context of molecular catalysts for the reactions involved in artificial photosynthesis.<sup>5</sup> However, further improvements are necessary to develop an applicable artificial photosynthesis device based on molecular components.

## Dye-sensitized photoelectrochemical cell combining a MOF catalyst and cobaltocene $\text{CoCpCp}^*$ as redox mediator for $\text{CO}_2$ reduction

Wojciech G. Sikorski,<sup>a</sup> Tianbo Duan,<sup>a</sup> Tijmen M. A. Bakker,<sup>a</sup> Joost N. H. Reek <sup>a</sup> and Jarl Ivar van der Vlugt <sup>ab</sup>

Creating a functional DS-PEC with a molecular catalyst involves addressing various challenges: (i) efficiency, (ii) heterogenization of catalytic material and (iii) engineering of an operational device.<sup>6</sup>

Metal-organic frameworks (MOFs) with embedded, well-defined molecular catalysts have been explored as electrochemical platforms for driving energy-relevant reactions, including carbon dioxide reduction.<sup>7</sup> Additionally, their potential in photocatalytic processes has been recognized, broadening their utility in energy conversion technologies.<sup>8</sup> PECs incorporating MOFs as semiconductor or light-harvesting material have recently garnered increasing interest within the scientific community.<sup>9</sup> However, currently, metal organic frameworks functionalized with embedded molecular catalysts are not broadly applicable in the context of designing efficient DS-PEC devices.

The main challenge is that incorporating a heterogenized molecular catalyst rooted within a MOF into a device with a photoelectrode necessitates careful consideration of the efficient transport of photogenerated electrons from the dye immobilized on the semiconductor to the catalytic sites within the MOF network. One potential solution involves introducing an external redox-active molecule (a redox mediator) to transport electrons from the photoelectrode to the catalytic sites within the MOF. In this configuration, the redox mediator facilitates electron transfer, which would otherwise depend on direct collisional interactions between the dye and the heterogenized catalyst. Consequently, electron transfer between the dye and the catalyst anchored within a MOF is limited by the diffusion of the redox mediator through the MOF framework.<sup>10</sup> Methyl viologen was recently used to mediate electron transfer from an electrode to otherwise electrochemically isolated catalytic sites within NU-1000 MOF to drive electrocatalytic hydrogen evolution, thereby showing that this is a feasible approach.<sup>11</sup> Application of the same concept in the photodriven reduction of  $\text{CO}_2$  is not known yet. We herein demonstrate that the new heteroleptic cobaltocene complex

<sup>a</sup> van 't Hoff Institute for Molecular Sciences, University of Amsterdam, Science Park 904, 1098 XH Amsterdam, the Netherlands

<sup>b</sup> Institute of Chemistry, Carl von Ossietzky University Oldenburg, Carl-von-Ossietzky-Str. 9-11, 26129 Oldenburg, Germany.  
E-mail: [jarl.ivar.van.der.vlugt@uni-oldenburg.de](mailto:jarl.ivar.van.der.vlugt@uni-oldenburg.de)



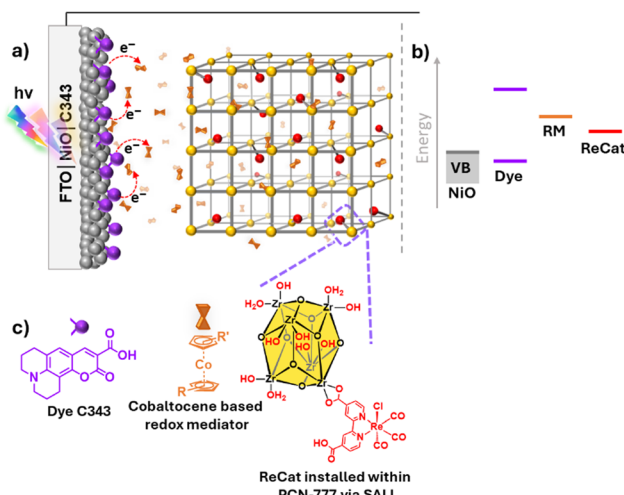


Fig. 1 Representation of a DS-MOF-PEC (cathodic part). (a) Charging of redox mediator at p-type dye-functionalized semiconductor and diffusion of former into **ReCat**@PCN-777; (b) energy levels of different components required for functioning of the cell, and (c) structure of the components within the cell.

$[\text{CoCpCp}^*]$  (**1**) is a competent redox mediator for  $\text{CO}_2$  reduction by a dye sensitized photoelectrochemical cell featuring the metal-organic framework PCN-777 functionalized with an embedded rhenium catalyst (**ReCat** –  $[\text{Re}(\text{4},\text{4}'-\text{bpydc})(\text{CO})_3\text{Cl}]$ ).<sup>12</sup> Hereafter referred to as DS-MOF-PEC, this system serves as an operational device for  $\text{CO}_2$  reduction (Fig. 1). The system represents a combination of a DSSC and a DS-PEC, as it integrates both a redox mediator and a catalyst. Species **1** has a redox potential above the potential of the photoexcited PS but below the onset potential for  $\text{CO}_2$  reduction with **ReCat**. Hence, it can facilitate electron transfer between the surface-anchored PS system and the catalytically active site embedded within the MOF framework.

The first stage of designing a functional DS-PEC involves determining and matching of the redox potentials of the cell's molecular components. The potential window for a redox mediator is thus guided by the potential at which **ReCat** catalyzes  $\text{CO}_2$  under electrocatalytic conditions (in  $\text{CO}_2$ -saturated acetonitrile), at  $-1.59$  V vs.  $\text{Fc}/\text{Fc}^+$  (see Fig. S11, SI) and the potential of coumarin-343 (**C343**) as the dye (acting as electron donor after photoexcitation) at  $-1.77$  V vs.  $\text{Fc}/\text{Fc}^+$ .<sup>13</sup> The molecular rhenium catalyst **ReCat** was incorporated in the mesoporous PCN-777 MOF *via* the SALI method. The content of rhenium within the MOF was evaluated by ICP-MS to be 1.80 weight percent. (see SI for details). Given the redox potentials of the dye and the catalyst, a suitable redox mediator should meet the following criteria: (1) be small enough to freely diffuse through the MOF scaffold to reach the catalytic rhenium sites buried within PCN-777, (2) possess a redox potential between  $-1.77$  V and  $-1.59$  V (vs.  $\text{Fc}/\text{Fc}^+$ ), to effectively transport electrons from the excited dye to **ReCat**, and (3) undergo reversible electrochemistry in order to serve as an electron shuttle between the photocathode and the catalyst. Based on these prerequisites, cobaltocene and derivatives thereof were

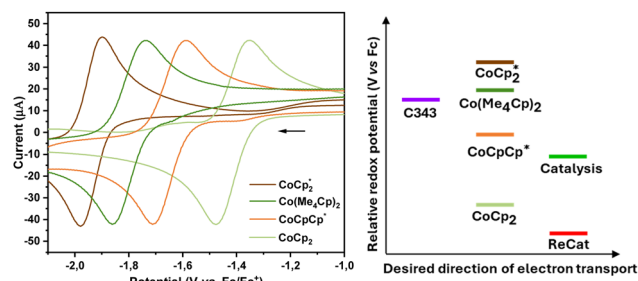


Fig. 2 Left: Cyclic voltammograms of cobaltocene derivatives (10 mM) in dry acetonitrile, (0.1 M TBAPF<sub>6</sub>) under Ar atmosphere, glassy carbon working electrode (Ø 3 mm), platinum wire/coil counter electrode (Ø 0.5 mm), Ag/AgCl reference electrode (in 3 M KCl), scan rate 100 mV s<sup>-1</sup>. Right: Redox potentials of molecular components used in DS-MOF-PEC.

considered as potentially adequate redox mediators. Cobaltocene itself is not a potent enough reducing agent to effectively transfer electrons to the rhenium catalyst, while bis( $\eta^5$ -pentamethylcyclopentadienyl)cobalt(II) ( $[\text{Co}(\text{Cp}^*)_2]$ ) is unsuitable as an electron acceptor for the photoexcited dye.<sup>14</sup> Introduction of methyl groups onto (one of) the Cp ligands was shown to effect the overall redox potential in ferrocene derivatives.<sup>15</sup> Translating this to cobaltocene chemistry, two new derivatives, *i.e.* heteroleptic  $\eta^5$ -cyclopentadienyl- $\eta^5$ -pentamethylcyclopentadienyl cobalt(II)  $[\text{CoCpCp}^*]$  (**1**) and homoleptic bis( $\eta^5$ -tetramethylcyclopentadienyl)cobalt(II)  $[\text{Co}(\text{Me}_4\text{Cp})_2]$  (**2**), were synthesized (see SI) and their redox potentials compared with those of cobaltocene and  $[\text{Co}(\text{Cp}^*)_2]$  (Fig. 2, left). Fig. 2 (right) illustrates the relative differences in redox potentials of the molecular components – photoexcited **C343**, cobaltocene-derived redox mediator and onset potential for **ReCat** – potentially to be used in the DS MOF-PEC (with the scale preserved for accuracy). Based on the electrochemical data, complex **1** is ideally suited as redox mediator for the envisioned DS MOF-PEC system.

Next, two separate experiments were carried out to ensure that the different components can indeed co-operate under  $\text{CO}_2$  reduction conditions. Firstly, sacrificial  $\text{CO}_2$  reduction was conducted using **ReCat**@PCN-777 and **1** in  $\text{CO}_2$ -saturated acetonitrile and with trifluoroethanol (TFE) as proton donor. Post-reaction analysis of the composition of the headspace in the gas-tight reaction vessel using gas chromatography (GC) revealed that this combination led to increased CO production compared to **ReCat** and **1**, while no CO was produced with only **ReCat**@PCN-777 (Table S3, Experimental section, SI). This is attributed to the suppression of inactive rhenium dimer formation, which is mitigated by anchoring of the catalyst within the MOF structure. The second is an evaluation of the photoelectrochemical properties of a photocathode consisting of FTO, NiO and a layer of **C343** in presence with complex **1**, *i.e.* to verify whether the electron generated by dye photoactivation can be transported by the Co-based redox mediator to the counter electrode, thereby generating photocurrent, using a DSSC set-up (Fig. S1, SI). This experiment confirmed the ability of the heteroleptic cobaltocene complex to act as electron

acceptor from the photoexcited and reductively quenched C343 dye.

Typically, both the reduced and oxidized form of a redox mediator are required for efficient DSSC performance, as oxidation and reduction processes occur simultaneously. For the commonly employed  $I_3^-/I^-$  redox couple, the presence of just 10 wt% of oxidized species ( $I_3^-$ ) was shown to effectively initiate electron transfer in a photoelectrochemical cell with mesoporous NiO electrode functionalized with C343 dye.<sup>16</sup> In this work, performance of the 'full' redox couple  $[\text{CoCp}_2]^{+}/[\text{CoCp}_2]$  was compared with a device containing only  $[\text{CoCp}_2]$ . In the experiment with the 'full' redox couple, photocurrent was observed immediately (Fig. 3). However, this enhanced photocurrent stopped abruptly after about 5 minutes, possibly due to the poisoning of NiO by  $\text{PF}_6^-$  anions, which was found to effect the valence band energy of NiO.<sup>17</sup> In contrast, with only  $\text{CoCp}_2$ , photocurrent rose after approx. 3 minutes, with the delay attributed to insufficient quantity of oxidized species at the start, limiting electron flow. Hence, these results indicate that the cobaltocenium ion can be generated *in situ*, and that once a sufficient concentration of this redox partner is reached, continuous photocurrent can be generated, although with a delayed response to light exposure.<sup>18</sup> Photocurrent does not increase with light intensity due to diffusion limitations of  $[\text{CoCp}_2]$  in the electrolyte.<sup>19</sup>

Thereafter, the chronoamperometry experiment was repeated with complex **1**. Photocurrent dropped rapidly during the stabilization period in the dark (900 s) and then remained stable for an extended period of time (Fig. S14, SI), indicating that the directional movement of charges reached equilibrium when an external voltage of 0 V was applied. When the light was alternated between on and off (after 900 seconds), photocurrent was generated instantaneously, increasing with light intensity and reaching approximately 0.04  $\mu\text{A}$  (Fig. 4).

This suggests that **1** is oxidized *in situ*, and that photocurrent is not constrained by the availability of cations, nor by the

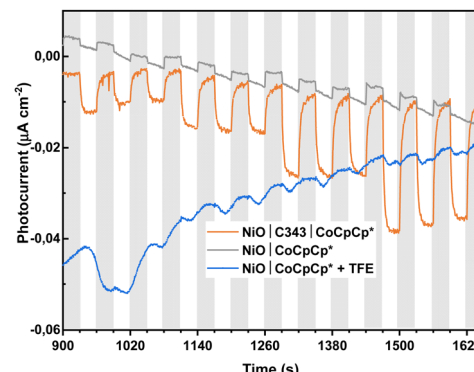


Fig. 4 Chopped light amperometry experiment with 10 mM of **1**, showing generated photocurrent upon illumination (from 900 seconds onwards). Control experiments in grey and blue. Cell was illuminated for periods of 30 seconds (indicated by white bars) by a white LED with  $100 \text{ mW cm}^{-2}$  intensity.

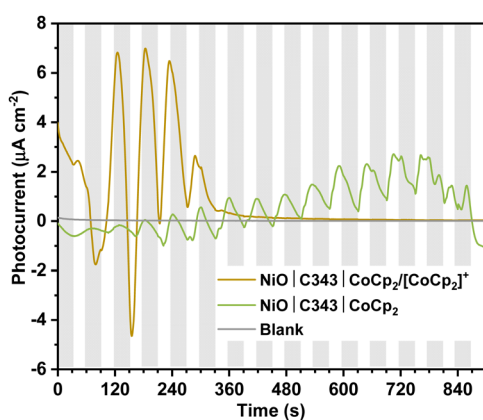


Fig. 3 Photocurrent generated in chopped light chronoamperometry experiment in a two-electrode cell with 10 mM of  $[\text{CoCp}_2]/[\text{CoCp}_2]^{+}$  (red) or only  $[\text{CoCp}_2]$  (green). Cell was illuminated for periods of 30 seconds (indicated by white bars) by white LED with  $100 \text{ mW cm}^{-2}$  intensity.

duration or intensity of illumination. Furthermore, as light intensity increased, the current did not return to zero, implying that the system does not revert to equilibrium and that net charge accumulation occurs on one side of the cell. The control experiment without C343 dye (Fig. 4, grey curve) confirmed that **1** is not photosensitive (and that the negligible photocurrent is associated with energy absorption and electron flow within the conduction band of NiO<sup>20</sup>). Lastly, to evaluate whether the proton source necessary for  $\text{CO}_2$  reduction could affect the performance of the whole system in the final device, a control experiment was performed in the presence of trifluoroethanol (TFE) (Fig. 4, blue curve). The results showed that TFE suppresses photocurrent. Attempts to analyze the mixture of **1** and TFE using NMR spectroscopy were unsuccessful, but it is reported that TFE can significantly alter the redox potential of ferrocene derivatives.<sup>21</sup> Therefore, separation of TFE from the NiO|C343|**1** components is critical.

The aforescribed observations indicate that integrating the FTO|NiO|C343 photocathode, complex **1**, and ReCat@PCN-777 into the final DS-MOF-PEC device should lead to a working device. Hence, all components were combined in a custom-designed DS-PEC reactor (Fig. S2, SI) and evaluated for photoelectrochemical  $\text{CO}_2$  reduction under continuous white LED illumination while monitoring the chronoamperometric response. The oxidative compartment of the cell, separated from the working compartment by a Nafion membrane, was loaded with the  $I_3^-/I^-$  redox couple and TFE as proton donor. The headspace of the reactor was analyzed by gas chromatography (GC) to determine the composition of the formed products. After a one-hour stabilization period, illumination with white LED light led to immediate generation of photocurrent, which stabilized at approximately  $15 \mu\text{A cm}^{-2}$  and persisted over 8 hours, until the light was turned off (Fig. 5, red line). Analysis of the reactor headspace using gas chromatography revealed the presence of CO – 13.6 units or  $0.55 \mu\text{mol}$ . The total electric current generated during the experiment was 451.2 mC, corresponding to  $4.68 \mu\text{mol}$  of electrons (see Fig. S5 and eqn (S1), SI). Given that  $\text{CO}_2$  reduction involves two



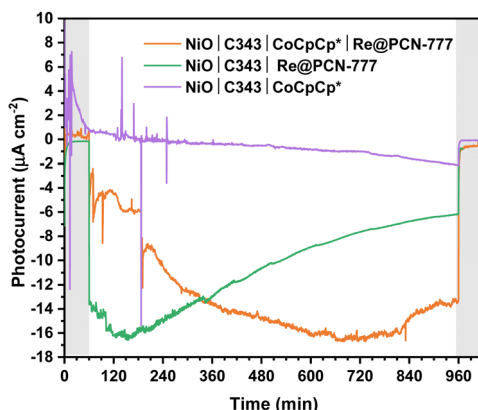


Fig. 5 Photocurrent, under white LED illumination ( $100 \text{ mW cm}^{-2}$ ) in MeCN, generated by DS-MOF-PEC assembled with NiO|C343 photocathode, CoCpCp\* (30  $\mu\text{mol}$ ) and Re@PCN-777 (0.29  $\mu\text{mol}$ ) and control experiments (without CoCpCp\* – green line; without Re@PCN-777 – purple line. Light was turned on after 60 min. of stabilization in dark and turned off after 15 hours (indicated by grey bars).

electrons, the amount of electrons used for this reaction was 1.10  $\mu\text{mol}$ , resulting in a faradaic efficiency of 24%. Permeation of  $I_3^-$  or  $I^-$  through the Nafion membrane (leading to (partial) consumption of generated electrons was ruled out by UV-Vis spectroscopy (see SI). A control experiment with no **1** present did not lead to any CO in the headspace, which validates the use of CoCpCp\* as a redox mediator and strongly indicates that this complex facilitates electron transfer between the photocathode and the heterogenized rhenium catalyst within the MOF.

This proof-of-concept research demonstrates the feasibility of utilizing the heteroleptic cobaltocene CoCpCp\* (**1**) as a redox mediator with the Re@PNC-777 catalyst in a dye-sensitized photoelectrochemical cell (DS-MOF-PEC) for  $\text{CO}_2$  reduction. The experiments confirm the effectiveness of **1** in facilitating electron transfer between the photocathode, consisting of FTO, NiO, and C343 dye, and the heterogenized rhenium catalyst (**ReCat**) incorporated into the PCN-777 framework. This configuration enables stable photocurrent generation under white LED illumination and successful CO production, validating the operational potential of the DS-MOF-PEC device. Control experiments underscore the essential role of CoCpCp\* as redox mediator and the requirement of **ReCat**@PCN-777 for effective catalytic activity. To the best of our knowledge, this study provides the first example demonstrating the integration of a heterogenized molecular catalyst embedded in a MOF structure for DS-PEC systems, advancing the development of efficient artificial photosynthesis devices for sustainable  $\text{CO}_2$  reduction.

Funding provided by the Dutch Research Council (NWO) via Mat4Sus Grant 7319.017.003 (CO<sub>2</sub>CatMat). Ed Zuidinga (MS) and Norbert Geels (BET) are thanked for technical assistance.

## Conflicts of interest

There are no conflicts to declare.

## Data availability

The data supporting this article have been included in the main article and as part of the SI.

Synthesis and characterization, electrochemical, analysis and photocatalysis data. See DOI: <https://doi.org/10.1039/d5cc01356a>

## Notes and references

1. D. Gust, T. A. Moore and A. L. Moore, *Acc. Chem. Res.*, 2009, **42**, 1890; J. W. Ager, M. R. Shaner, K. A. Walczak, I. D. Sharp and S. Ardo, *Energy Environ. Sci.*, 2015, **8**, 2811; D. F. Bruggeman, T. M. A. Bakker, S. Mathew and J. N. H. Reek, *Chem. – Eur. J.*, 2021, **27**, 218.
2. J. Li and N. Wu, *Catal. Sci. Technol.*, 2015, **5**, 1360.
3. M. Grätzel, *Nature*, 2001, **414**, 338.
4. Z. Yu, F. Li and L. Sun, *Energy Environ. Sci.*, 2015, **8**, 760; J. Gong, K. Sumathy, Q. Qiao and Z. Zhou, *Renewable Sustainable Energy Rev.*, 2017, **68**, 234; M. Kyu Kim and H. Kyu Kim, *ACS Omega*, 2023, **8**, 6139.
5. B. Zhang and L. Sun, *Chem. Soc. Rev.*, 2019, **48**, 2216; N. Nandal and S. L. Jain, *Coord. Chem. Rev.*, 2022, **451**, 214271; X. Li, Z. Yu, C. Zhang, B. Li, X. Wu, Y. Liu and Z. Zhu, *Small Methods*, 2024, 2400683.
6. T. Bouwens, T. M. A. Bakker, K. Zhu, J. Hasenack, M. Dieperink, A. M. Brouwer, A. Huijser, S. Mathew and J. N. H. Reek, *Nat. Chem.*, 2023, **15**, 213; E. Marchini, S. Caramori and S. Carli, *Molecules*, 2024, **29**, 293.
7. N. F. Suremann, B. D. McCarthy, W. Gschwind, A. Kumar, B. A. Johnson, L. Hammarström and S. Ott, *Chem. Rev.*, 2023, **123**, 6545; J.-M. Huang, X.-D. Zhang, J.-Y. Huang, D.-S. Zheng, M. Xu and Z.-Y. Gu, *Coord. Chem. Rev.*, 2023, **494**, 215333.
8. S. Navalón, A. Dhakshinamoorthy, M. Álvaro, B. Ferrer and H. García, *Chem. Rev.*, 2022, **123**, 445; M. Stanley, J. Haimerl, N. B. Shustova, R. A. Fischer and J. Warnan, *Nat. Chem.*, 2022, **14**, 1342.
9. B. Gibbons, M. Cai and A. J. Morris, *J. Am. Chem. Soc.*, 2022, **144**, 17723; B. Chen, Z. Yang, Q. Jia, R. J. Ball, Y. Zhu and Y. Xia, *Mater. Sci. Eng. R: Rep.*, 2023, **152**, 100714.
10. C. H. Sharp, B. C. Bukowski, H. Li, E. M. Johnson, S. Illic, A. J. Morris, D. Gersappe, R. Q. Snurr and J. R. Morris, *Chem. Soc. Rev.*, 2021, **50**, 11530.
11. H. Noh, C.-W. Kung, K. Otake, A. W. Peters, Z. Li, Y. Liao, X. Gong, O. K. Farha and J. T. Hupp, *ACS Catal.*, 2018, **8**, 9848.
12. J. Hawecker, J.-M. Lehn and R. Ziessl, *J. Chem. Soc., Chem. Commun.*, 1983, **9**, 539.
13. A. Morandeira, G. Boschloo, A. Hagfeldt and L. Hammarström, *J. Phys. Chem. C*, 2008, **112**, 9530.
14. B. Hwang, M.-S. Park and K. Kim, *ChemSusChem*, 2015, **8**, 310; N. G. Connelly and W. E. Geiger, *Chem. Rev.*, 1996, **96**, 877.
15. A. Paul, R. Borrelli, H. Bouyanfif, S. Gotts and F. Sauvage, *ACS Omega*, 2019, **4**, 14780.
16. H. Zhy, A. Hagfeldt and G. Boschloo, *J. Phys. Chem. C*, 2007, **111**, 17455.
17. Z.-X. She and S.-H. Yang, *RSC Appl. Interfaces*, 2024, **1**, 443.
18. D. F. Bruggeman, T. M. A. Bakker, S. Mathew and J. N. H. Reek, *Chem. – Eur. J.*, 2021, **27**, 218.
19. A. Lewandowski, L. Waligora and M. Galinski, *J. Solution Chem.*, 2013, **42**, 251.
20. L. D'Amario, G. Boschloo, A. Hagfeldt and L. Hammarström, *J. Phys. Chem. C*, 2014, **118**, 19556.
21. I. Noviandri, K. N. Brown, D. S. Fleming, P. T. Gulyas, P. A. Lay, A. F. Masters and L. Phillips, *J. Phys. Chem. B*, 1999, **109**, 6713.

